NANO LETTERS

2009
Vol. 9, No. 12
4172-4176

Raman Spectroscopy of Ripple Formation in Suspended Graphene

Chun-Chung Chen,[†] Wenzhong Bao,[‡] Jesse Theiss,[†] Chris Dames,[§] Chun Ning Lau,[‡] and Stephen B. Cronin*[,†]

Department of Electrical Engineering, University of Southern California, Los Angeles, California 90089, and Department of Physics and Astronomy and Department of Mechanical Engineering, University of California, Riverside, California 92521

Received July 24, 2009; Revised Manuscript Received September 3, 2009

ABSTRACT

Using Raman spectroscopy, we measure the optical phonon energies of suspended graphene before, during, and after thermal cycling between 300 and 700 K. After cycling, we observe large upshifts (~25 cm^{-1}) of the G band frequency in the graphene on the substrate region due to compression induced by the thermal contraction of the underlying substrate, while the G band in the suspended region remains unchanged. From these large upshifts, we estimate the compression in the substrate region to be ~0.4%. The large mismatch in compression between the substrate and suspended regions causes a rippling of the suspended graphene, which compensates for the change in lattice constant due to the compression. The amplitude (*A*) and wavelength (λ) of the ripples, as measured by atomic force microscopy, correspond to an effective change in length $\Delta l/l$ that is consistent with the compression values determined from the Raman data.

The mechanical instability of graphene is one of its most interesting properties.[1−3] Ripple formation in suspended and on-substrate graphene has been demonstrated both experimentally[4−6] and theoretically,[7−9] though with much variation in character and orientation. Furthermore, these ripples have been shown to create midgap states and charge inhomogeneity in the graphene.[10,11] Therefore, a method of producing well-ordered graphene ripples will help provide a deeper understanding of these structures and their electrical, magnetic, and mechanical properties. Recently, Bao et al. developed a method for forming well-ordered ripples in a controllable fashion by the thermal cycling of suspended graphene.[12] The period and amplitude of these ripples were satisfactorily accounted for by a classical elasticity theory model, which correlated well with the thickness of the suspended graphene.

Raman spectroscopy provides a very precise measure of the vibrational energies of carbon nanotubes and graphene, which respond very sensitively to changes in strain and compression. As such, Raman spectroscopy provides a good tool for characterizing the strain and compression in these nanoscale systems.[13,14] Cronin et al. were able to observe changes in the Raman spectra of carbon nanotubes for strains as small as $\varepsilon = 0.1\%$.[15,16] Huang et al. measured the Raman spectra of graphene under uniaxial strains of a few percent.[17] They observed downshifts in the G and 2D bands of $\partial\omega_G/\partial\varepsilon = -12.5\ cm^{-1}/\%$ and $\partial\omega_{2D}/\partial\varepsilon = -21\ cm^{-1}/\%$, respectively. Similarly, Mohiuddin et al. studied graphene under uniaxial and biaxial strain both experimentally and theoretically.[18] They reported values of the strain-induced downshifts of the G band of $\partial\omega_G/\partial\varepsilon = -30\ cm^{-1}/\%$ and $\partial\omega_G/\partial\varepsilon = -58\ cm^{-1}/\%$ for uniaxial and biaxial strain, respectively. This biaxial strain coefficient is consistent with recent measurements under hydrostatic pressure.[19]

Here, we present the first Raman spectroscopy measurements of periodic ripple formation in suspended graphene before and after thermal cycling. These ripples arise from the compression induced in graphene due to the difference in thermal expansion coefficients between graphene and the underlying silicon substrate. This compression is quantified by measuring the change in the G band Raman frequency, while the amplitude and wavelength of the ripples are measured by atomic force microscopy (AFM).

Graphene membranes, ranging from single layers (0.35 nm) to multiple layers (2 nm) in thickness, and 0.5 to 20 μm in width, are deposited suspended across predefined trenches on Si/SiO_2 substrates using mechanical exfoliation.[20] Spatially resolved micro-Raman spectra are collected in a Renishaw inVia micro-Raman spectrometer, while the temperature is varied in a Linkam THMS temperature-controlled stage. In this work, a 532 nm, 5 W Spectra Physics solid state laser is collimated and focused through a Leica *DM*LM

[†] Department of Electrical Engineering, University of Southern California.
[‡] Department of Physics and Astronomy, University of California, Riverside.
[§] Department of Mechanical Engineering, University of California, Riverside.

10.1021/nl9023935 CCC: $40.75
Published on Web 10/06/2009

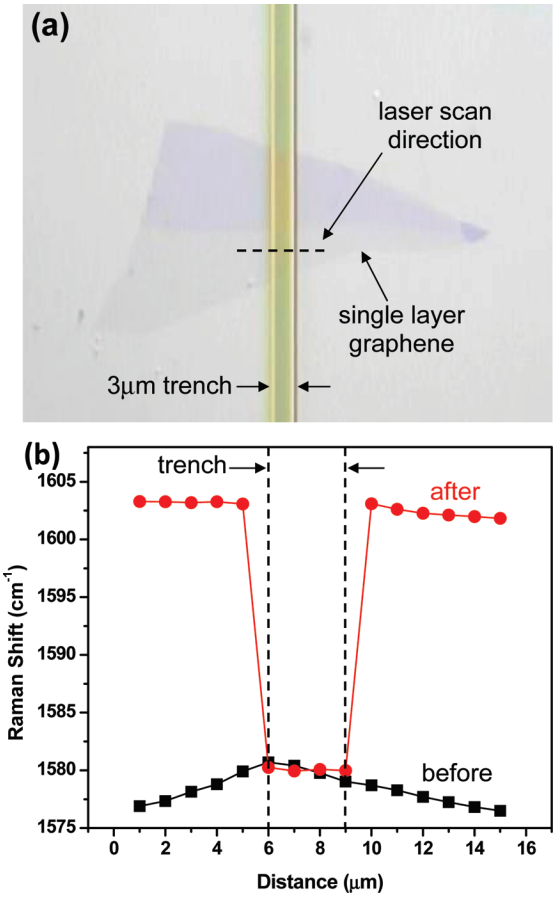

Figure 1. (a) Optical microscope image of a graphene single layer suspended over a 3 μm trench. (b) Spatial mapping of the G band Raman shift taken perpendicular to the trench before and after thermal cycling to 700 K.

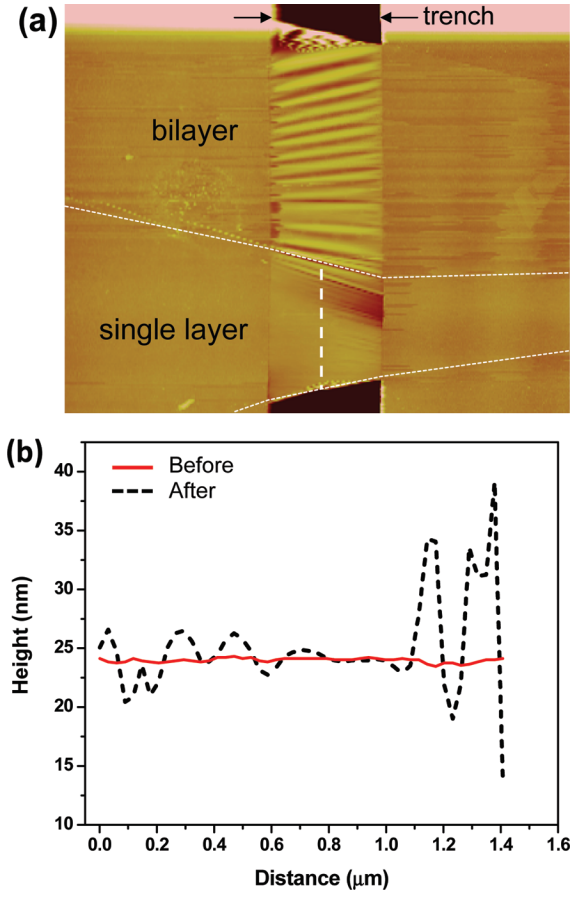

Figure 2. Atomic force microscope (a) image and (b) cross-sectional analyses of the suspended graphene single layer shown in Figure 1 (a) before and (b) before and after thermal cycling to 700 K.

microscope and used to irradiate these samples with a 100X objective lens with NA = 0.9, working distance = 0.3 mm, and spot size = 0.5 μm. All measurements were performed in air under standard atmospheric conditions.

Figure 1a shows an optical microscope image of a graphene single layer suspended over a 3 μm trench. Spatial mappings of the G band Raman shift taken before and after thermal cycling to 700 K are shown in Figure 1b at the locations indicated by the dashed line in Figure 1a. Before thermal cycling, a slight upshift in the Raman frequency can be seen in the trench region. This indicates either a small compression in the suspended region or, more likely, a small strain in the substrate region. After thermal cycling, however, a large upshift of $\Delta\omega_G = 25$ cm^{-1} is observed in the substrate region, while the trench region remains unchanged, indicating the presence of significant compression in the single layer graphene on the substrate. Such compression arises from the differential thermal expansion between graphene and the substrate, in particular, from the negative thermal expansion of graphene.[12]

The biaxial compression of the graphene on the substrate is manifested differently for the suspended portion of the graphene. Because the bending energy of the thin membrane is much smaller than the potential energy induced by changing bond lengths, the compressive strain in the suspended graphene is relieved by the formation of ripples, as shown in Figure 2. In the ideal case where the ripples can be approximated as a sinusoid with amplitude (A) and wavelength (λ), the effective contraction of the graphene is given by

$$\Delta l = \int \mathrm{d}l = \int \left(\sqrt{1 + \left[\frac{2\pi}{\lambda} A \cos\left(\frac{2\pi x}{\lambda} \right) \right]^2} - 1 \right) \mathrm{d}x$$

$$\varepsilon = \frac{\Delta l}{l} = (\pi A/\lambda)^2 + O(A/\lambda)^4$$

where we have used a Taylor series expansion to obtain the final form. Figure 2 shows an AFM topography image and cross-section analyses of the suspended graphene before and after thermal cycling. Before heating, the graphene appears flat. However, after thermal cycling, ripples can be seen. In order to accurately analyze these real ripple patterns, which deviate significantly from the sinusoidal idealization, we evaluate the actual change in length $\Delta l/l$ using the AFM software (DI, Nanoscope) to be 0.40%, which is in good agreement with the compression value determined from the Raman upshifts shown in Figure 1, as described below. From the AFM cross-section data, we determine the average amplitude and wavelength of these ripples to be 5.2 nm and 0.26 μm, respectively.

Spatially mapped Raman spectra were taken after every 100 K increment during heat-up and cool-down and are

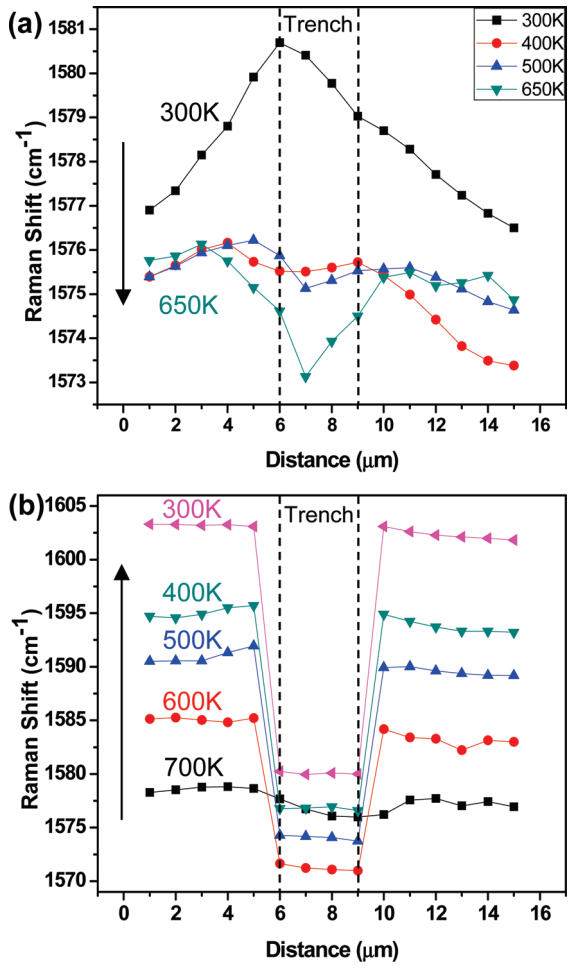

Figure 3. Raman spatial maps taken during (a) heat up to 650 K and (b) cool down from 700 K.

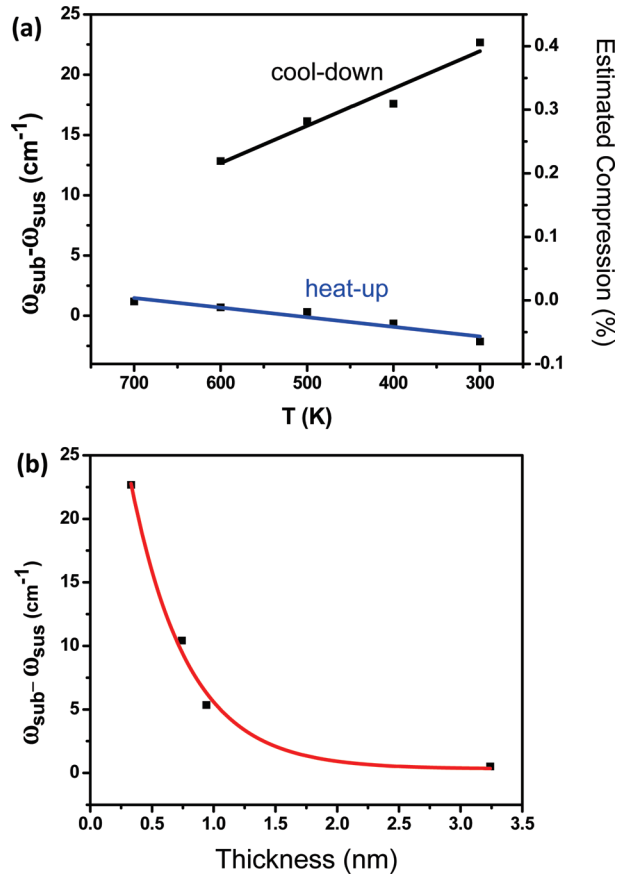

Figure 4. (a) Difference between the average G band Raman shift of the suspended and substrate regions and estimated biaxial compression taken during thermal cycling. (b) Raman upshift between the substrate and suspended regions plotted as a function of graphene thickness.

shown in Figure 3. According to the observations of Bao et al. during the thermal cycling, the suspended graphene samples became taut at temperatures higher than 600 K due to the thermal expansion of the underlying substrate and the thermal contraction of the graphene.[12] Subsequent cooling from 700 to 300 K creates compression and ripples in the graphene samples. In our Raman measurements, the G band Raman frequency of the suspended graphene in the trench region was roughly equal to that measured in the substrate region during heat-up (Figure 3a). During cool-down, however, the Raman frequencies of the suspended and substrate regions begin to deviate significantly due to the compression induced by the thermal contraction of the silicon substrate and the thermal expansion of the graphene (Figure 3b). After thermal cycling, the Raman upshift observed in the substrate region relative to the suspended region was $\omega_{sub} - \omega_{sus} = 22.7$ cm^{-1}. The first principles calculations of Mohiuddin et al. predict downshifts of $\partial\omega_G/\partial\varepsilon = -58$ cm^{-1}/% for biaxial strain.[18] Assuming this coefficient for both tension and compression,[19] we estimate a compression of 0.39% from the 22.7 cm^{-1} upshift observed in our work after thermal cycling. This value of compression agrees well with the value obtained from AFM. We note these frequency shifts are much larger than those that could be explained by the temperature dependence of the Raman peaks alone, which follow $(\partial\omega)/(\partial T)|_\varepsilon \approx -0.016$ cm^{-1}/K according to ref 21. As mentioned above, the relatively small variations in the Raman frequency along the length of the graphene before and during heat-up indicate some slight strain induced during mechanical exfoliation or by the thermal expansion of the trench. Figure 4a shows the difference in the average Raman frequency between the substrate and suspended regions ($\omega_{sub} - \omega_{sus}$), plotted as a function of temperature as the sample is thermally cycled between 300 and 700 K. The data are found to follow a linear dependence on temperature. The biaxial compression estimated from Mohiuddin's work is also shown in the figure on the right axis.

Spatially mapped Raman spectra and AFM data were taken before, during, and after thermal cycling on a total of four suspended graphene samples. Table 1 summarizes these results. Samples 1 and 2 showed Raman upshifts of $\Delta\omega_G = 22.7$ and 10.4 cm^{-1} and estimated compressions of 0.39% and 0.18%, respectively, based on the theoretical predictions of Mohuiddin et al.[18] These results are consistent with the effective compressions obtained from the AFM data, 0.4% and 0.25%, respectively. Sample 3 shows results for a graphene trilayer that exhibits a somewhat smaller Raman upshift and compression after thermal cycling. Unfortunately, no AFM data could be obtained from this sample after thermal cycling. Sample 4 shows data from a multilayered

Table 1. Raman and AFM Data Summary of Four Samples before and after Thermal Cycling

sample	graphene layers	graphene thickness (nm)	max temp (T_{max}) (K)	Raman upshift after cycling ($\omega_{sub} - \omega_{sus}$) ($cm^{-1}$)	compression estimated from Raman upshift (%)	effective compression ($\Delta l/l$) from AFM data (%)
1	single layer	0.33	700	22.7	0.39	0.40
2	bilayer	0.74	700	10.4	0.18	0.25
3	triple layer	0.94	700	5.3	0.09	N/A
4	multiple layer	3.24	700	0.5	0.01	0.058

sample of graphene, which exhibits a significantly lower value of Raman-estimated and AFM-estimated compression. Figure 4b shows a plot of the relative upshift of the G band after thermal cycling ($\omega_{sub} - \omega_{sus}$) plotted as a function of the graphene thickness. A clear trend can be seen in the sample thickness dependence of the Raman upshift, which is consistent with the observations of Proctor et al. under hydrostatic pressure.[19] This plot clearly shows that the graphene thickness plays a significant role in the compression created by thermal cycling, such that thinner graphene samples experience more compression than thicker graphene samples.

The thermal expansion coefficient (TEC) of graphene can be estimated from our measurements. Carbon nanostructure materials are known to exhibit an anomalous (negative) thermal expansion coefficient.[22−24] Here, we observe a compression of 0.4% over a 400 K (1×10^{-5}/K) temperature difference, which arises from the difference in thermal expansion coefficients of graphene and the underlying silicon. Subtracting the TEC due to the underlying silicon substrate (4.7×10^{-6}/K)[12,25] gives a value of -5.3×10^{-6}K for the TEC of single layer graphene. This is consistent with the values given in our previous work, verifying the classical elasticity theory model used to interpret those results.[12] This value is much larger in magnitude than the TEC of graphite in the basal plane, -1×10^{-6}/K, and roughly one and a half times larger than the value predicted for graphene from theoretical calculations.[24]

We note that Berciaud et al. have also observed significant shifts in the Raman spectra of suspended graphene relative to on-substrate graphene.[26] However, in that work, the shifting of these Raman peaks was attributed to a doping effect, which is known to cause upshifts and line width narrowing of the G band in graphene through the blockage of the decay channel of phonons into electron−hole pairs.[27−29] A spatial mapping of the G band Raman line width of the suspended graphene sample shown in Figure 1 taken before and after thermal cycling to 700 K is shown in the online supporting document.[30] The data show a broadening of the G band line width in the suspended region, which can be explained by inhomogeneous broadening. Since the period of the ripples is smaller than the laser spot, local variations in the Raman frequency will be spatially averaged over the collection area (laser spot), resulting in a broadened Raman line width after the ripples are formed. The on-substrate graphene, however, shows a narrowing of the G band line width from approximately 13 to 9 cm^{-1}, which may indicate doping due to charge transfer from the underlying substrate. However, the doping required to achieve this line width narrowing is relatively small and corresponds to upshifts of just several cm^{-1}.[29] Another alternative is that a compression-induced band gap is created.[13,14,31,32] If the band gap is larger than the G band phonon energy, it will block the decay of phonons into electron−hole pairs, causing the observed upshift and line width narrowing. Further studies must be conducted in order to separate these possible effects. The additional topographical information provided by AFM corroborates the existence of compression, which we believe is the primary effect on the observed Raman spectra.

In conclusion, we observe significant upshifts in the Raman spectra of suspended graphene (25 cm^{-1}) after thermal cycling treatment (300−700−300 K). For single layer graphene, these upshifts correspond to compressions in the substrate region up to 0.4% and ripple formation in the suspended region of the graphene. The effective change in length, as determined from AFM measurements of the ripple amplitude and wavelength, is consistent with the values of compression estimated from the Raman upshifts. These independent measurements verify that the ripples originate from the change in lattice constant in the compressed region. Lastly, the thickness dependence of the compression induced by thermal cycling was ascertained and was found to decrease with increasing graphene thickness.

Acknowledgment. This research was supported in part by DOE Award No. DE-FG02-07ER46376 and NSF Award No. CBET-0854118. W.B. and C.N.L. acknowledge the support by NSF/CAREER DMR/0748910, ONR N00014-09-1-0724, and ONR/DMEA H94003-09-2-0901. C.N.L. and C.D. acknowledge the support by NSF/CBET 0854554.

Supporting Information Available: A figure showing spatial mapping of the G band Raman linewidth of the suspended graphene sample shown in Figure 1 taken before and after thermal cycling to 700 K. This material is available free of charge via the Internet at http://pubs.acs.org.

References

(1) Mermin, N. D. Crystalline Order in 2 Dimensions. *Phys. Rev.* **1968**, *176*, 250.
(2) Booth, T. J.; Blake, P.; Nair, R. R.; Jiang, D.; Hill, E. W.; Bangert, U.; Bleloch, A.; Gass, M.; Novoselov, K. S.; Katsnelson, M. I.; Geim, A. K. Macroscopic graphene membranes and their extraordinary stiffness. *Nano Lett.* **2008**, *8*, 2442–2446.
(3) Novoselov, K. S.; Jiang, D.; Schedin, F.; Booth, T. J.; Khotkevich, V. V.; Morozov, S. V.; Geim, A. K. Two-dimensional atomic crystals. *Proc. Natl. Acad. Sci. U.S.A.* **2005**, *102*, 10451–10453.
(4) Geringer, V.; Liebmann, M.; Echtermeyer, T.; Runte, S.; Schmidt, M.; Ruckamp, R.; Lemme, M. C.; Morgenstern, M. Intrinsic and extrinsic corrugation of monolayer graphene deposited on SiO_2. *Phys. Rev. Lett.* **2009**, *102*, 076102.
(5) Deshpande, A.; Bao, W.; Miao, F.; Lau, C. N.; LeRoy, B. J. Spatially resolved spectroscopy of monolayer graphene on SiO_2. *Phys. Rev. B* **2009**, *79*, 205411.

(6) Borca, B.; Calleja, F.; Hinarejos, J. J.; de Parga, A. L. V.; Miranda, R. Reactivity of periodically rippled graphene grown on Ru(0001). *J. Phys.: Condens. Matter* **2009**, *21*, 134002.
(7) Fasolino, A.; Los, J. H.; Katsnelson, M. I. Intrinsic ripples in graphene. *Nat. Mater.* **2007**, *6*, 858–861.
(8) Shenoy, V. B.; Reddy, C. D.; Ramasubramaniam, A.; Zhang, Y. W. Edge-Stress-Induced Warping of Graphene Sheets and Nanoribbons. *Phys. Rev. Lett.* **2008**, *101*, 245501.
(9) Tang, C.; Meng, L. J.; Sun, L. Z.; Zhang, K. W.; Zhong, J. X. Molecular dynamics study of ripples in graphene nanoribbons on 6H-SiC(0001): Temperature and size effects. *J. Appl. Phys.* **2008**, *104*, 113536.
(10) de Parga, A. L. V.; Calleja, F.; Borca, B.; Passeggi, M. C. G.; Hinarejos, J. J.; Guinea, F.; Miranda, R. Periodically rippled graphene: Growth and spatially resolved electronic structure. *Phys. Rev. Lett.* **2008**, *100*, 046403.
(11) Guinea, F.; Katsnelson, M. I.; Vozmediano, M. A. H. Midgap states and charge inhomogeneities in corrugated graphene. *Phys. Rev. B* **2008**, *77*, 17003.
(12) Bao, W.; Miao, F.; Chen, Z.; Zhang, H.; Jang, W.; Dames, C.; Lau, C. N. Spontaneous and Thermally Controlled Rippling of Suspended Graphene Atomic Membranes. *Nat. Nanotechnol.* **2009**, *4*, 562−566.
(13) Ni, Z. H.; Yu, T.; Lu, Y. H.; Wang, Y. Y.; Feng, Y. P.; Shen, Z. X. Uniaxial Strain on Graphene: Raman Spectroscopy Study and Band-Gap Opening. *ACS Nano* **2008**, *2*, 2301–2305.
(14) Yu, T.; Ni, Z. H.; Du, C. L.; You, Y. M.; Wang, Y. Y.; Shen, Z. X. Raman mapping investigation of graphene on transparent flexible substrate: The strain effect. *J. Phys. Chem. C* **2008**, *112*, 12602–12605.
(15) Cronin, S. B.; Swan, A. K.; Unlu, M. S.; Goldberg, B. B.; Dresselhaus, M. S.; Tinkham, M. Measuring the uniaxial strain of individual single-wall carbon nanotubes: Resonance Raman spectra of atomic-force-microscope modified single-wall nanotubes. *Phys. Rev. Lett.* **2004**, *93*, 167401.
(16) Cronin, S. B.; Swan, A. K.; Unlu, M. S.; Goldberg, B. B.; Dresselhaus, M. S.; Tinkham, M. Resonant Raman spectroscopy of individual metallic and semiconducting single-wall carbon nanotubes under uniaxial strain. *Phys. Rev. B* **2005**, *72*, 035425.
(17) Huang, M. Y.; Yan, H. G.; Chen, C. Y.; Song, D. H.; Heinz, T. F.; Hone, J. Phonon softening and crystallographic orientation of strained graphene studied by Raman spectroscopy. *Proc. Natl. Acad. Sci. U.S.A.* **2009**, *106*, 7304–7308.
(18) Mohiuddin, T. M. G.; Lombardo, A.; Nair, R. R.; Bonetti, A.; Savini, G.; Jalil, R.; Bonini, N.; Basko, D. M.; Galiotis, C.; Marzari, N.; Novoselov, K. S.; Geim, A. K.; Ferrari, A. C. Uniaxial strain in graphene by Raman spectroscopy: G peak splitting, Gruneisen parameters, and sample orientation. *Phys. Rev. B* **2009**, *79*, 8.
(19) John E. Proctor, E. G., Konstantin S. Novoselov, Mustafa Lotya, Jonathan N. Coleman, Matthew P. Halsal, Graphene under hydrostatic pressure. *Phys. Rev. B*, in press.
(20) Novoselov, K. S.; Geim, A. K.; Morozov, S. V.; Jiang, D.; Zhang, Y.; Dubonos, S. V.; Grigorieva, I. V.; Firsov, A. A. Electric field effect in atomically thin carbon films. *Science* **2004**, *306*, 666–669.
(21) Calizo, I.; Balandin, A. A.; Bao, W.; Miao, F.; Lau, C. N. Temperature dependence of the Raman spectra of graphene and graphene multilayers. *Nano Lett.* **2007**, *7*, 2645–2649.
(22) Kwon, Y. K.; Berber, S.; Tomanek, D. Thermal contraction of carbon fullerenes and nanotubes. *Phys. Rev. Lett.* **2004**, *92*, 015901.
(23) Schelling, P. K.; Keblinski, R. Thermal expansion of carbon structures. *Phys. Rev. B* **2003**, *68*, 035425.
(24) Mounet, N.; Marzari, N. First-principles determination of the structural, vibrational and thermodynamic properties of diamond, graphite, and derivatives. *Phys. Rev. B* **2005**, *71*, 205214.
(25) Watanabe, H.; Yamada, N.; Okaji, M. Linear thermal expansion coefficient of silicon from 293 to 1000 K. *Int. J. Thermophys.* **2004**, *25*, 221–236.
(26) Berciaud, S.; Ryu, S.; Brus, L. E.; Heinz, T. F. Probing the Intrinsic Properties of Exfoliated Graphene: Raman Spectroscopy of Free-Standing Monolayers. *Nano Lett.* **2009**, *9*, 346–352.
(27) Das, A.; Pisana, S.; Chakraborty, B.; Piscanec, S.; Saha, S. K.; Waghmare, U. V.; Novoselov, K. S.; Krishnamurthy, H. R.; Geim, A. K.; Ferrari, A. C.; Sood, A. K. Monitoring dopants by Raman scattering in an electrochemically top-gated graphene transistor. *Nat. Nanotechnol.* **2008**, *3*, 210–215.
(28) Ni, Z. H.; Yu, T.; Luo, Z. Q.; Wang, Y. Y.; Liu, L.; Wong, C. P.; Miao, J. M.; Huang, W.; Shen, Z. X. Probing Charged Impurities in Suspended Graphene Using Raman Spectroscopy. *ACS Nano* **2009**, *3*, 569–574.
(29) Pisana, S.; Lazzeri, M.; Casiraghi, C.; Novoselov, K. S.; Geim, A. K.; Ferrari, A. C.; Mauri, F. Breakdown of the adiabatic Born-Oppenheimer approximation in graphene. *Nat. Mater.* **2007**, *6*, 198–201.
(30) Online Supporting Document for Chun-Chung Chen, et al., Raman Spectroscopy of Ripple Formation in Suspended Graphene.
(31) Zhou, S. Y.; Gweon, G. H.; Fedorov, A. V.; First, P. N.; De Heer, W. A.; Lee, D. H.; Guinea, F.; Neto, A. H. C.; Lanzara, A. Substrate-induced bandgap opening in epitaxial graphene. *Nat. Mater.* **2007**, *6*, 770–775.
(32) Giovannetti, G.; Khomyakov, P. A.; Brocks, G.; Kelly, P. J.; van den Brink, J. Substrate-induced band gap in graphene on hexagonal boron nitride: Ab initio density functional calculations. *Phys. Rev. B* **2007**, *76*, 073103.

NL9023935